ISBN: 978-981-18-5852-9
WCSE 2022 Spring Event: 2022 9th International Conference on Industrial Engineering and Applications
doi: 10.18178/wcse.2022.04.017

Day-ahead Optimal Scheduling of Integrated Energy Systems Considering Photovoltaic and Demand Response Uncertainties

Ronghua Zhang [1], Jianjie Li [2] Peng Li [3] Huacan Lv [4] and Chengfu Wang [5]

[1, 2, 3] Binzhou Power Suply Company
State Grid Shandong Electric Power Company
Binzhou, China
[4. 5] School of Electrical Engineering
Shandong University
Jinan, China

Abstract. The uncertainty of photovoltaic and demand response brings challenges to the optimal scheduling of integrated energy system (IES) in the market circumstances. In this paper, the uncertainty model of photovoltaic and demand response is firstly established. On this basis, an optimal scheduling strategy based on interval linear stochastic chance constrained programming is proposed. The uncertainty of renewable energy generation prediction is described by probability distribution function, and the uncertainty of load participating demand response is described by interval number. Thus, an interval linear stochastic chance constraint programming model is constructed, and the model is solved by Cplex solver. The proposed method is compared with the interval linear programming and stochastic chance constrained programming models used separately in IES. The results show that the proposed method has lower operating cost and less dependence on the prediction accuracy, and can improve the economy of IES while ensuring the safe operation of the system.

Keywords: integrated energy system; uncertainty of source and load; day-ahead scheduling; interval linear stochastic chance constrained programming; demand response

1. Introduction

The gradual exhaustion of fossil energy and the increasingly serious environmental pollution make the efficient use of energy become imperative. The application of renewable energy, energy marketization and multi-energy interconnection have become the focus of scholars to promote clean and efficient use of energy [1-3].

Compared with the traditional single electric energy utilization mode, the integrated energy system (IES) [4-6] realizes the flexible transformation and unified management of different energy with the help of advanced conversion and storage equipment [7-8]. It provides a new solution for promoting the absorption of renewable energy and improving the operation economy of the system. In terms of promoting the absorption of renewable energy, [9] proposes a double-layer optimal scheduling model for IES considering the conversion of electricity to gas. And it proves that the conversion of electricity to gas can effectively improve the absorption capacity of wind power of the power grid through case analysis. In terms of improving system running economy, [10] studies the IES optimization scheduling method, and it establishes the electricity as the core of IES optimization scheduling model, as the scheduling model by using particle swarm optimization algorithm, verify that subsystems of IES can complement each other to effectively increase the efficiency.

This work is supported by the Science and Technology Project of Shandong Electric Power Company, State Grid. (Project Name: Research on collaborative operation method of Regional Integrated Energy System adapting to Multi-dimensional and High-order Uncertain Renewable energy Access Project; ERP Code: 520615210004).

However, most of the above research only study the optimization of IES from the perspective of source and network, without considering the potential effects of various demand side management (DSM) measures that may exist in the actual situation. In the actual integrated energy system, system operators can guide users to actively adjust their own energy consumption and participate in demand response (DR) by virtue of advanced information and communication technology, thus effectively improving the flexibility of system operation [11]. In view of this, [12] analyzes the contribution of demand response in IES to improving the economy and flexibility of the system based on cold, heat and electricity loads. [13] reveals the influence of DR on system investment income by establishing a sustainable planning model of IES.

At present, most studies on IES only focus on deterministic systems without considering the influence of various uncertainties in practical engineering. In fact, for IES including renewable energy, the randomness, intermittency of power generation and the fluctuation of various loads lead to the existence of multiple uncertainties, which makes it impossible to predict the power generation and load accurately. Therefore, it is impossible to make an accurate dispatching plan for the system, which has a great impact on the stability and economy of the operation of IES.

Based on the above background, this paper takes IES as the research object, which is composed of renewable energy, heat and electricity load and other uncertain units, power grid, cogeneration unit, electricity storage system, heat storage system, gas boiler and other controllable energy supply and consumption units. In addition, aiming at the economic operation of the system, the uncertainty of photovoltaic and demand response is modelled, and the source-load uncertainty optimization model based on interval linear stochastic chance constraint programming is established. Finally, an example is given to verify the feasibility and rationality of the proposed method.

2. Source-load Uncertainty Model

2.1. Uncertainty of Photovoltaic Power Generation

Studies show that photovoltaic power is affected by solar irradiance, weather type, season and ambient temperature [14]. The randomness of weather factors makes the prediction error of photovoltaic power also randomness. According to the inference of the central limit theorem, data obtained by simple random sampling generally obey normal distribution [15]. Relevant studies have shown that the prediction error of renewable energy conforms to normal distribution [16].

Therefore, the photovoltaic prediction error is considered to be normal distribution in this study. Assume that the prediction error of the random variable renewable energy power generation power is ΔP_{pv}, the error expectation is 0, and the variance is σ_{pv}^2. The probability density function of the prediction error is shown in (1).

$$f(\Delta P_{pv}) = \frac{1}{\sqrt{2\pi}\sigma_{pv}} e^{-\frac{\Delta P_{pv}^2}{2\sigma_{pv}^2}} \tag{1}$$

2.2. Uncertainty of Loads Involved in Demand Response

The uncertainty of demand response is mainly reflected in the uncertainty of the loads involved in the demand response. In actual engineering systems, users' willingness to use energy is determined by psychological factors and living habits, so it is difficult to establish the probability distribution function accurately [17]. Therefore, the interval method is used in this paper to describe the predicted value of electrical load and heat load, as shown in (2) and (3).

$$[P_{eload}^n] = P_{eload}^n[1-\beta_e, 1+\beta_e], \beta_e \in [0,1] \tag{2}$$

$$[H_{hload}^n] = H_{hload}^n[1-\beta_h, 1+\beta_h], \beta_h \in [0,1] \tag{3}$$

Where, the symbol [] represents interval number or interval variable. P_{eload}^n , H_{hload}^n are respectively the predicted value of electrical load and thermal load of the energy hub n; β_e, β_h are respectively the relative prediction error of electrical load and thermal load.

3. Demand Response Mechanism Modelling

Demand response can optimize the load curve by guiding users to change their energy consumption behavior through price, so as to mobilize the flexibility of the load side and reduce the energy supply pressure during peak energy consumption periods. Price signals can be divided into time-of-use (tOU) price and peak-valley price according to the time scale [18]. In this paper, tOU price is adopted to fine-analyze the impact of demand response on scheduling operation.

The power load after demand response can be obtained as follows:

$$P_{eload}^{n} = P_{eload0}^{n} + \Delta P_{eload}^{n} \tag{4}$$

Where, P_{eload0}^{n} is the pre-response power load demand; ΔP_{eload}^{n} is the change of power load after the implementation of demand response, which has the following relationship with the change of tOU price:

$$\Delta P_{eload,NOR}^{n} = E\Delta e_{NOR} \tag{5}$$

$$\Delta P_{eload,NOR}^{n} = [\frac{\Delta P_{eload,1}^{n}}{P_{eload0,1}^{n}} \quad \frac{\Delta P_{eload,2}^{n}}{P_{eload0,2}^{n}} \quad \cdots \quad \frac{\Delta P_{eload,T}^{n}}{P_{eload0,T}^{n}}]^{T} \tag{6}$$

$$\Delta e_{NOR} = [\frac{\Delta e_1}{e_1^0} \quad \frac{\Delta e_2}{e_2^0} \quad \cdots \quad \frac{\Delta e_T}{e_T^0}]^{T} \tag{7}$$

Where, $\Delta P_{eload,NOR}^{n}$ is the normalized matrix of power load change; Δe_{NOR} is the normalized matrix of tOU price changes; E is the elasticity matrix of electricity price; $P_{eload0,i}^{n}$ and e_i^0 are the original power demand and tOU price of time period respectively; $\Delta P_{eload,i}^{n}$ and Δe_i are respectively the changes of power demand and tOU price before and after the implementation of demand response; Δe is the change of tOU price before and after the demand response; T is the total number of scheduling periods.

Loads can be classified according to the degree to which they are affected by price. The price elasticity parameters of various loads are determined by comparing the demand - price changes at the same time after the base date and time-sharing price. In this paper, the self-elasticity coefficient of electricity is set as -0.1 by referring to the analysis data of the American industrial department [19].

4. Day-ahead Economic Scheduling Considering Source - load Uncertainty

The IES in this paper mainly includes photovoltaic power generation devices, combined heat and power (CHP) units, gas boiler (GB) and Electric boiler (EB), and they are connected to the main power grid to meet the thermal and electrical load requirements of users. The specific structure is shown in the fig.1:

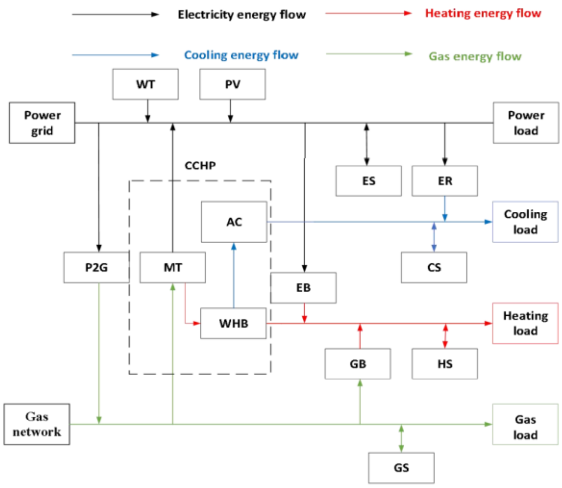

Fig. 1. Structure of IES.

In this paper, a day-ahead optimization scheduling model of IES based on interval linear stochastic chance constraint programming is established, considering the stochastic chance constraint programming of photovoltaic output uncertainty and the interval linear programming of participating in demand response load uncertainty.

4.1. The Objective Function

Taking economic optimization as the optimization objective, the objective function of the optimization scheduling model is set as the operating cost of the comprehensive energy system within a single scheduling cycle, as shown in (8).

$$[C_{\text{total}}] = \min\left([C_{\text{E}}]+[C_{\text{CHP}}]+[C_{\text{GB}}]\right) \tag{8}$$

Where, $[C_{\text{total}}]$ is the interval number of the total operating cost within the scheduling period of the integrated energy system; $[C_{\text{E}}]$ is the interval number of power purchase cost from large grid; $[C_{\text{CHP}}]$ is the interval number of CHP unit start-up and shutdown and operation cost; $[C_{\text{GB}}]$ is the interval number of GB operating cost.

The purchase cost of large power grid is shown in (9).

$$[C_{\text{E}}] = \sum_{k=1}^{T}[P_{\text{Grid}}(k)]\cdot c_{\text{Grid}}(k)\cdot\Delta t \tag{9}$$

Where, k is the specific time period of the scheduling cycle, T is the number of time periods of a single scheduling cycle, and can be set to 24 for day-ahead scheduling. $[P_{\text{Grid}}(k)]$ and $c_{\text{Grid}}(k)$ are the interval number and price of power purchased from the large grid in the k period respectively; Δt is a single scheduling period.

The start-up and operation costs of CHP units are shown in (10).

$$\begin{aligned}[C_{\text{CHP}}] = {} & S_{\text{U,D}}^{\text{CHP}}\cdot\left|\delta_{\text{CHP}}(1,1)-B\right| + S_{\text{U,D}}^{\text{CHP}}\cdot\sum_{k=2}^{T}\left(\left|\delta_{\text{CHP}}(k-1)-\delta_{\text{CHP}}(k)\right|\right)+ \\ & \sum^{T}\left\{\left\{a\cdot[P_{\text{CHP}}(k)]+b\cdot[H_{\text{CHP}}(k)]+c\cdot\delta_{\text{CHP}}(k)\right\}\cdot\Delta t\right\}\end{aligned} \tag{10}$$

Where, $S_{\text{U,D}}^{\text{CHP}}$ is the single start-up and shutdown cost of CHP unit; B is the operating status of the CHP unit at the last moment on the scheduling day; $\delta_{\text{CHP}}(k)$ is the operating status of CHP unit in the period k, where 1 stands for running and 0 stands for stopping. $\delta_{\text{CHP}}(k)$ and $[H_{\text{CHP}}(k)]$ are the interval numbers of generation power and heat generation power of the CHP unit in the period k; A, B and c are linear fuel cost coefficients of CHP unit.

GB operating cost is shown in (11).

$$[C_{\text{GB}}] = \sum_{k=1}^{T}\left(c_{\text{gas}}\cdot\frac{[H_{\text{GB}}(k)]}{\eta_{\text{GB}}}\cdot\Delta t\right) \tag{11}$$

Where, c_{gas} is the natural gas cost coefficient; η_{GB} is the heat generation efficiency of GB; $[H_{\text{GB}}(k)]$ is the interval number of GB heat generation power in the period k.

4.2. The Constraints

I. Power constraints of IES

Power constraint of IES includes balance constraint of electric power and thermal power. The electric power balance constraint is shown in (12).

$$\begin{aligned}\Pr\Big\{ & [P_{\text{Gird}}(k)]+[P_{\text{CHP}}(k)]+\delta_{\text{E,c}}(k)\cdot[Q_{\text{E,c}}(k)]- \\ & \delta_{\text{E,d}}(k)\cdot[Q_{\text{E,d}}(k)]+P_{\text{Renew}}(k)+\Delta P_{\text{Renew}}(k) \\ & =[P_{\text{e,EB}}(k)]+\sum_{m=1}^{M}[P_{\text{e, load}}^{m}(k)]\Big\}\geq\beta\end{aligned} \tag{12}$$

Where, Pr{·} is the probability of the establishment of constraint conditions; β is the given confidence level; $[P_{\text{e,EB}}(k)]$ and $[P_{\text{e, load}}^{m}(k)]$ are respectively the interval number of EB input power of electric boiler and electric load of the energy hub n in the k period; $P_{\text{Renew}}(k)$ is Photovoltaic power of renewable energy in the period k; Represents the prediction error of renewable energy photovoltaic power generation in period k; $\Delta P_{\text{Renew}}(k)$ is a random variable, and its probability distribution function is given in (1).

Thermal power balance constraint is shown in (13).

$$
\begin{aligned}
&\left[H_{\mathrm{CHP}}(k)\right]+\delta_{\mathrm{T,c}}(k)\cdot\left[Q_{\mathrm{T,c}}(k)\right]- \\
&\delta_{\mathrm{T,d}}(k)\cdot\left[Q_{\mathrm{T,d}}(k)\right]+\eta_{\mathrm{EB}}\cdot\left[P_{\mathrm{e,EB}}(k)\right]+\left[H_{\mathrm{GB}}(k)\right] \\
&=\sum_{m=1}^{M}\left[H_{\mathrm{h,load}}^{m}(k)\right]+\left[H_{\mathrm{h,loss}}(k)\right]
\end{aligned}
\tag{13}
$$

Where, $\delta_{\mathrm{T,c}}(k)$ and $\delta_{\mathrm{T,d}}(k)$ are the binary variables of TSS charging and releasing state in period k respectively; $\left[Q_{\mathrm{T,c}}(k)\right]$ and $\left[Q_{\mathrm{T,d}}(k)\right]$ are the interval numbers of TSS heat charge and release power in period k; η_{EB} is the heat generation efficiency of EB; $\left[H_{\mathrm{h,load}}^{m}(k)\right]$ and $\left[H_{\mathrm{h,loss}}(k)\right]$ are respectively the number of heat load interval of building m and the number of total heat loss power interval of the building in period k.

II. Constraints on CHP unit operation

$$
\begin{cases}
\max\{c_{\lambda 2}\cdot\left[H_{\mathrm{CHP}}(k)\right]+P_{\mathrm{CHP}}^{\min}, \\
\qquad \lambda\cdot\left\{\left[H_{\mathrm{CHP}}(k)\right]-H_0\right\}\}\le\left[P_{\mathrm{CHP}}(k)\right] \\
0\le\left[H_{\mathrm{CHP}}(k)\right]\le H_{\mathrm{CHP}}^{\max}
\end{cases}
\tag{14}
$$

Where, $P_{\mathrm{CHP}}^{\max}$ and $P_{\mathrm{CHP}}^{\min}$ are respectively the maximum and minimum power of the CHP unit under pure coagulation condition; $H_{\mathrm{CHP}}^{\max}$ is the maximum heat generation power of CHP unit; $c_{\lambda 1}$ and $c_{\lambda 2}$ are the slope of condensing unit curve; λ is the curve slope of the back pressure unit; H_0 is the heat threshold of the work done by the steam driven steam turbine of the back pressure unit.

III. Power constraints of GB, EB and main grid connection line

$$0\le\left[H_{\mathrm{GB}}(k)\right]\le H_{\mathrm{GB}}^{\max} \tag{15}$$

$$0\le\left[P_{\mathrm{e,EB}}(k)\right]\le P_{\mathrm{EB}}^{\max} \tag{16}$$

$$0\le\left[P_{\mathrm{Grid}}(k)\right]\le P_{\mathrm{Grid}}^{\max} \tag{17}$$

Where, $H_{\mathrm{GB}}^{\max}$ is the maximum heat generation power of GB; $P_{\mathrm{EB}}^{\max}$ is the maximum input power of EB; $P_{\mathrm{Grid}}^{\max}$ is the maximum purchased power of the integrated energy system.

4.3. Model Performance Index

In this paper, the operating cost fluctuation index is used to conduct a comparative study on the uncertain model and the deterministic model, as shown in (18).

$$\varepsilon=\frac{\left(f_{\mathrm{u}}^{+}+f_{\mathrm{u}}^{-}\right)/2-f_{\mathrm{c}}}{f_{\mathrm{c}}}\times 100\% \tag{18}$$

Where, ε is the fluctuation index of the operating cost of the interval model; f_{c} is the operating cost of the determined model; f_{u}^{+} and f_{u}^{-} are respectively the upper and lower limits of the interval number of the operating cost of the interval model.

4.4. Model Solution

The optimal scheduling model of IES constructed in this paper is essentially an interval linear random chance constrained programming model. Firstly, the model is decomposed into two sub-models, and then the opportunity constraint conditions in the sub-models are transformed into definite equivalent conditions. The original model is replaced by the optimal sub model and the worst sub model after transformation, and the optimal value of each sub model is obtained respectively, so as to obtain the optimal value range. The solution method of the model refers to the enhanced interval linear programming method [19] and the interval credibility opportunity constrained programming method [29].

5. The Case Studies

The IES constructed in this paper includes 5-node network [20] and 6-node thermal network [21]. Thermal network loss parameters, TSS parameters, CHP unit operating characteristic interval parameters [22] and ESS parameters details as references.

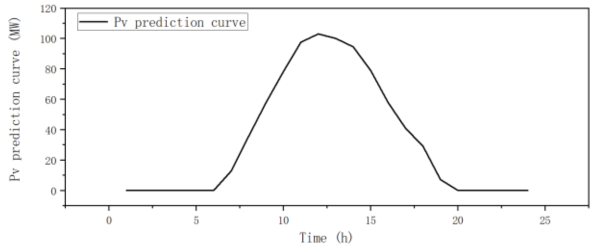

Fig. 2. Photovoltaic forecast data.

Photovoltaic forecast data curve is shown in Figure 2. The thermal and electrical load prediction data of typical buildings are shown in Figure 3. Power purchase price and unit calorific value price of natural gas are provided in [15]

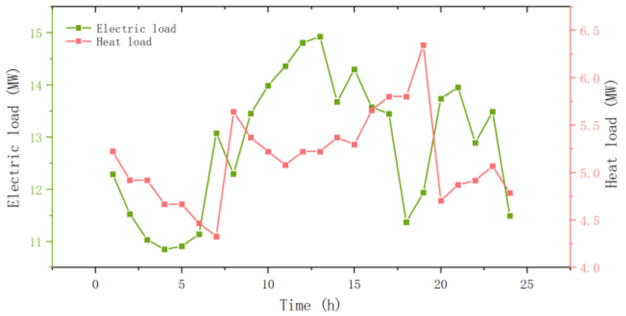

Fig. 3. Electrical and thermal load data.

5.1. Analysis of Demand Response Results

For demand response, the relationship model between tOU price and electricity load is established.

Fig. 4 shows the total load curve before and after the demand response. After the demand response, the load fluctuation is suppressed to a certain extent, the trough load increases and the peak load decreases. This is because through demand response, the peak load is transferred to the trough period, which promotes the effective transportation of energy. Thus, power flow congestion is alleviated and the system is not operated in the less efficient peak hours.

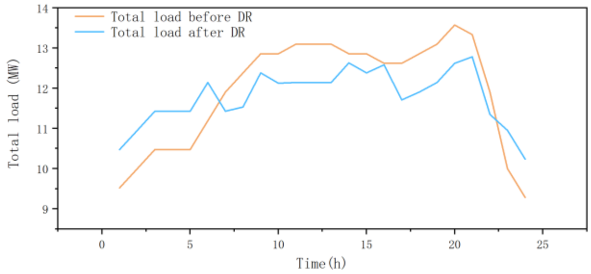

Fig. 4. Load before and after DR.

The figure below shows tOU price before and after demand response. The price difference of time-sharing energy expands further after the demand response, that is, the valley electricity price decreases and the peak electricity price increases. This encourages users to use less energy in peak times and more energy in trough times, and the scheme of social energy use becomes more efficient.

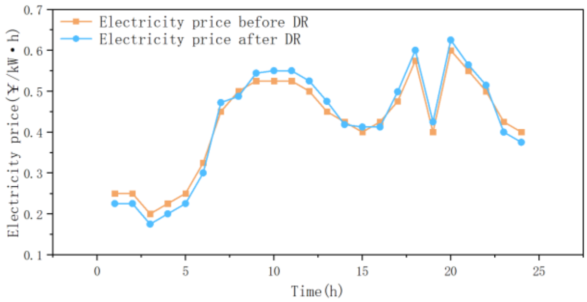

Fig. 5. Electrical price before and after DR.

5.2. Analysis of Uncertain Results

Three cases are presented for comparative analysis.

1) Model 1. Considering only photovoltaic uncertainty, stochastic chance constrained programming is used.

2) Model 2. Considering both photovoltaic and load uncertainties, stochastic chance constrained programming is used.

3) Model 3(proposed in this paper). Considering both photovoltaic and load uncertainties, interval linear random chance constrained programming is used.

Fig.6 shows the fluctuation indices of system operating costs in model 1, model 2 and model 3 at different confidence levels. The increase of confidence level means that the constraint ability of the system to meet the equilibrium condition is stronger, and the predicted value of the random variables in the model must be reduced accordingly to meet the requirements. In model 2, both photovoltaic and load uncertainties are dealt with by stochastic chance constraint programming method, and the proportion of load random variable is higher than photovoltaic random variable, so the fluctuation index changes in a downward trend and the range of variation is larger. Both model 1 and model 3 use stochastic chance constraint programming to deal with photovoltaic uncertainty, so the fluctuation index has the same trend.

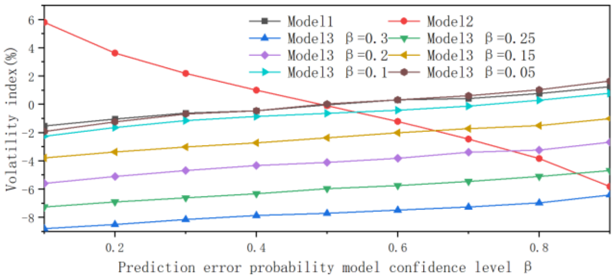

Fig. 6. Operating cost volatility index β.

Model 1 does not consider the uncertainty of load, while model 3 adopts interval linear programming method to deal with the uncertainty of load. At the same confidence level, the fluctuation index decreases with the increase of relative error of load prediction, and the overall economy of this case is higher than that of model 1. For load forecasting model of $\alpha = 0.05$ in model 3, the volatility index features largely consistent with the model 2, and the volatility index change range is smaller than model 1. Compared with model 1, which only considers photovoltaic uncertainty, model 3 not only considers photovoltaic and load uncertainty, but also has a smaller range of cost fluctuation than model 2. The model has lower dependence on prediction accuracy and higher stability.

6. Conclusion

Under the background of Energy Internet, multiple uncertainties such as renewable energy generation and the prediction error of participating demand response load are considered in IES. Based on stochastic chance constraint programming and interval linear programming, a day-ahead economic scheduling model of IES based on interval linear chance constraint programming is established. The results show that compared with the traditional scheduling model which only considers single uncertainty or only uses one method to deal with multiple uncertainties, the proposed interval linear stochastic chance constraint programming model is superior. While considering multiple uncertainties, it uses different processing methods for different characteristics of uncertainties, which reduces the dependence on prediction accuracy and improves the operation economy of the system. In addition to the uncertainties of new energy output, users' own energy consumption and demand prediction, there are still uncertainties such as random failures of capacity equipment/energy conversion equipment/energy transmission equipment, short-term energy market price changes, and even the impact of weather on heat generation/storage efficiency. These uncertainties are coupled to some extent, so it is necessary to model the uncertainty of comprehensive demand response reasonably. This is also the focus of future research in this paper.

7. References

[1] J. Hao et al., "A Heat Current Model for Heat Transfer/Storage Systems and Its Application in Integrated Analysis and Optimization With Power Systems," IEEE Transactions on Sustainable Energy, vol. 11, no. 1, pp. 175-184, Jan. 2020.

[2] C. Jiang and X. Ai, "Study on Optimal Operation of Integrated Energy System Considering New Energy Incentive Mechanism," in Proc. 2019 IEEE 3rd Conference on Energy Internet and Energy System Integration (EI2), 2019, pp. 301-306.

[3] Z. Guo, G. Li, M. Zhou and W. Feng, "Resilient Configuration Approach of Integrated Community Energy System Considering Integrated Demand Response Under Uncertainty," IEEE Access, vol. 7, pp. 87513-87533, 2019.

[4] N. Liu, J. Wang and L. Wang, "Hybrid Energy Sharing for Multiple Microgrids in an Integrated Heat–Electricity Energy System," IEEE Transactions on Sustainable Energy, vol. 10, no. 3, pp. 1139-1151, July 2019.

[5] L. Chen, Z. Li. Scenario-based optimal reserve dispatch considering uncertainty of wind power, China International Journal of Smart Grid and Clean Energy, vol. 3, no. 2, pp. 228-233, April 2014.

[6] L. Cheng, T. Yu, H. Jiang, S. Shi, Z. Tan and Z. Zhang, "Energy internet access equipment integrating cyber-physical systems: concepts, key technologies, system development, and application prospects," IEEE Access, vol. 7, pp. 23127-23148, 2019.

[7] Y. Xu et al,. "Multi-agent inday joint optimization scheduling of regional integrated energy system based on comprehensive demand response and Game," The Grid Technology, vol. 43, no. 7, pp.2506-2518.2019.

[8] H. Yang, M. Li, Z. Jiang and P. Zhang, "Multi-Time Scale Optimal Scheduling of Regional Integrated Energy Systems Considering Integrated Demand Response," IEEE Access, vol. 8, pp. 5080-5090, 2020.

[9] Z. Zeng, T. Ding, Y. Xu, Y. Yang and Z. Dong, "Reliability Evaluation for Integrated Power-Gas Systems With Power-to-Gas and Gas Storages," IEEE Transactions on Power Systems, vol. 35, no. 1, pp. 571-583, Jan. 2020.

[10] L. Gan-yun, C. Bin, J. De-xiang, W. Nan, L. Jun and C. Guangyu, "Optimal scheduling of regional integrated energy system considering integrated demand response," CSEE Journal of Power and Energy Systems, 2020.

[11] C. Eksin, H. Deliç and A. Ribeiro, "Demand Response Management in Smart Grids With Heterogeneous Consumer Preferences," IEEE Transactions on Smart Grid, vol. 6, no. 6, pp. 3082-3094, Nov. 2015.

[12] A. Karapetyan et al., "A Competitive Scheduling Algorithm for Online Demand Response in Islanded Microgrids," IEEE Transactions on Power Systems, vol. 36, no. 4, pp. 3430-3440, July 2021.

[13] F. Alfaverh, M. Denaï and Y. Sun, "Demand Response Strategy Based on Reinforcement Learning and Fuzzy Reasoning for Home Energy Management," IEEE Access, vol. 8, pp. 39310-39321, 2020.

[14] I. A. Ibrahim, M. J. Hossain and B. C. Duck, "An Optimized Offline Random Forests-Based Model for Ultra-Short-Term Prediction of PV Characteristics," IEEE Transactions on Industrial Informatics, vol. 16, no. 1, pp. 202-214, Jan. 2020.

[15] A. Ahmadi, M. Nabipour, B. Mohammadi-Ivatloo, A. M. Amani, S. Rho and M. J. Piran, "Long-Term Wind Power Forecasting Using Tree-Based Learning Algorithms," IEEE Access, vol. 8, pp. 151511-151522, 2020.

[16] T. Hu, W. Wu, Q. Guo, H. Sun, L. Shi and X. Shen, "Very short-term spatial and temporal wind power forecasting: A deep learning approach," CSEE Journal of Power and Energy Systems, vol. 6, no. 2, pp. 434-443, June 2020.

[17] S. Kumari, H. Karn, L. Varshney, L. Garg and N. Kumari, "Energy Management Strategy for Cost Minimization under Time of Use Pricing for Residential Application," 2020 IEEE International Students' Conference on Electrical,Electronics and Computer Science (SCEECS), pp. 1-4, 2020.

[18] H. Yang, L. Wang, Y. Zhang, H. -M. Tai, Y. Ma and M. Zhou, "Reliability Evaluation of Power System Considering Time of Use Electricity Pricing," IEEE Transactions on Power Systems, vol. 34, no. 3, pp. 1991-2002, May 2019, 3.

[19] N. Liu, J. Wang and L. Wang, "Hybrid Energy Sharing for Multiple Microgrids in an Integrated Heat–Electricity

Energy System," IEEE Transactions on Sustainable Energy, vol. 10, no. 3, pp. 1139-1151, July 2019.

[20] S. Zhang, W. Gu, S. Yao, S. Lu, S. Zhou and Z. Wu, "Partitional Decoupling Method for Fast Calculation of Energy Flow in a Large-Scale Heat and Electricity Integrated Energy System," IEEE Transactions on Sustainable Energy, vol. 12, no. 1, pp. 501-513, Jan. 2021.

[21] J. Li, M. Zhu and Y. Huang, "Classification and location scheme selection of coupling components in integrated electrical and heating systems with renewable energy," CSEE Journal of Power and Energy Systems, vol. 6, no. 3, pp. 619-629, Sept. 2020.

[22] Y. Wang et al., "Optimal Scheduling of the Regional Integrated Energy System Considering Economy and Environment," IEEE Transactions on Sustainable Energy, vol. 10, no. 4, pp. 1939-1949, Oct. 2019.